"imbalance" hypothesis for induction of emphysema by proteolytic injury to the lung extracellular matrix (ECM), is supported by animal experimental data (11,12). However, this hypothesis may not fully explain the loss of lung tissue that occurs in emphysema induced by cigarette smoking. Recently, alveolar cell apoptosis, which involves vascular endothelial cell growth factor (VEGF)-mediated signaling (13-17), (18), has been recognized as playing a key role in the progression of emphysema (19). VEGF induces angiogenesis and endothelial cell growth; withdrawal of VEGF leads to endothelial cell apoptosis *in vitro* and *in vivo* (20,21). Blockade of the VEGF receptor-2 (VEGFR-2) in rats through chronic administration of a chemical inhibitor, resulted in increased alveolar size and septal cell apoptosis without changing the inflammatory cell profile (14). In addition, biopsies of human emphysema tissue revealed decreased expression of VEGF and VEGFR-2, and increased apoptosis of both alveolar epithelia and endothelial cells (13). Consistent with these results, expression of ceramide was shown to be increased in patients with emphysema (16).

The present study explored mechanisms, other than dysregulation of TGF-β1 receptor activation, of emphysema development in *Fut8*$^{-/-}$ mice. Based on biochemical and genetic studies, it was concluded that the suppression of VEGFR-2 expression may play a role in the pathogenesis of emphysema in *Fut8*$^{-/-}$ mice.

Materials and methods

Cell lines

The human alveolar epithelial cell carcinoma line, A549, was maintained in Dulbecco's modified Eagle's medium (DMEM) supplemented with 10% fetal bovine serum (FBS), 50 units/ml of penicillin and 50 μg/ml streptomycin with antibiotics in 5% CO_2 at 37 °C. The mouse pancreatic acinar cell carcinoma line, TGP49, was maintained in DMEM:Ham's F12 (1:1) medium

supplemented with 10% FBS, 2 mM glutamine and antibiotics in 5% CO_2 at 37°C.

Mice

The Fut8-/- mice were established as previously described (6). F1 heterozygous were mated with C57BL/6 mice to produce the F2-generation mice that were used in that study. Therefore, these mice had ~75 of C57BL/6 genetic background. However, the mice survival rates were dramatically decreased after backcross. In fact, we found that mice, which have ~93 of C57BL/6 genetic background (F4-generation mice), rarely lived longer than one month. In this study, we used mice with ~87 of C57BL/6 genetic background (F3-generation mice). The survival rate of these mice was less than 10% at postnatal day 3. The wild-type mice were littermates of Fut8-/- mice at different ages.

Assay of Fut8 activity

The specific activity of Fut8 was determined using a synthetic substrate, 4-(2-pyridylamino)-butyl-amine (PABA)-labeled oligosaccharide. Subconfluent cells were washed once with PBS (-), and the cell pellet was suspended in 200 µl lysis buffer containing 10 mM Tris-HCl (pH 7.4), 150 mM NaCl and 1% Triton X-100. Fut8 activity in the cell lysate was assayed as described previously (22).

Immunohistochemical analysis

To detect the VEGFR-2 and Ceramide, whole lung tissues from animals after age indicated were fixed in 0.1 M phosphate buffer containing 4% paraformaldehyde and embedded in paraffin. For immunohistochemical analysis, the dewaxed sections were pretreated with Avidin-Biotin Blocking, Hydroxygen Blocking (DAKO, Glostrup, Denmark) for 10 min at 37 °C and then

incubated with mouse monoclonal anti-ceramide antibody (MID 15B4; Axxora, LLC., San Diego, CA), and mouse monoclonal anti-VEGFR-2 (A-3; Santa Cruz Biotechnology, Santa Cruz, CA) for 16 h at 4 °C. Localization of the first antibody was visualized by an avidin-biotin coupling (ABC) immunoperoxidase technique using a commercial kit (Vectastain Elite ABCTM; Vector Laboratories, Burlingame, CA), according to the instructions of the manufacturer. The immunostainings were taken by morphometric analysis, using a microscope system (Microphot F-XA; NIKKON, Tokyo, Japan) and application (Photograb-250; FujiFilm, Tokyo, Japan).

Western blot analysis

Cells, or tissues, were solubilized in 1% Triton X-100 lysis buffer (20 mM Tris-HCl (pH7.4), 10 mM EGTA, 10 mM $MgCl_2$, 1 mM benzamidine, 60 mM β-glycerophosphate, 1mM Na_3VO_4, 20 mM NaF, 2 g/ml aprotinin, 5 μg/ml leupeptin, 0.1 mM PMSF), and then centrifuged at 15,000 *g* for 15 min. The supernatants were collected, and protein concentrations were determined using a BCA protein assay (Pierce, Rockford, IL). Equal amounts of protein were run on 10 % or 8% SDS-PAGE gels under reducing conditions. The separated proteins were then transferred to PVDF membranes (Millipore Corporation, Bedford, MA). The blots were probed with anti-Flk-1 (VEGFR-2) (Santa Cruz, CA), anti-EGFR (Upstate Biotechnology, Lake Placid, NY), or anti-TGFβ receptor type II (Upstate Biotechnology) antibodies. Immunoreactive bands were visualized using an ECL kit (Amersham Pharmacia Biotech, UK). The membranes were stripped and re-probed with anti-β-actin antibody (Santa Cruz, CA) to confirm equal loading.

Immunoprecipitation

Cells were homogenized in lysis buffer as described above, and the cell lysates were centrifuged at 15,000 *g* for 15 min. The supernatant (~3 mg) was pre-cleared using 30 μl protein G-Sepharose

(50% slurry) and then incubated with anti-VEGFR-2 antibody. The immunoprecipitate was washed three times with lysis buffer. Equal amounts of protein were subjected to 7.5 % SDS-PAGE for Western blot analysis.

Terminal transferase dUTP nick end-labeling (TUNEL) assay

TUNEL staining was performed using a DeadEnd™ Colorimetric TUNEL System (Promega, Madison, WI), following the manufacturer's instructions. Briefly, after deparaffinization and dehydration, sections were washed with 0.85% NaCl and fixed with 10% buffered formalin in PBS. Sections were digested with proteinase K (20 μg/ml) for 10 min. After washing with PBS, sections were fixed with 10% buffered formalin in PBS a second time and then were soaked in equilibration buffer for 10 min. The sections were incubated with rTdT reaction mixture at 37 ℃ for 60 minutes. After the reaction was stopped with 2 x SSC buffer, endogenous peroxidase activity was quenched with 0.3% hydrogen peroxide. After incubation with streptavidin HRP solution (1:500), the sections were washed with PBS, immersed in diaminobenzidine (DAB) solution, and then observed using a light microscope.

Construction of the siRNA vector and retroviral infection

A retroviral vector carrying siRNA (sense: 5'-UCUCAGAAUUGGCGCUAUGTT-3', anti-sense: 3'-TTAGAGUCUUAACCGCGCGAUAC-5') targeted to Fut8 was constructed as previously described (23). Briefly, A 21-nuleotide sequence of Fut8 gene was inserted in the sense and anti-sense directions into the pSINsi-mU6 cassette vector containing the mouse U6 promoter (Takara Bio). The retroviral supernatant was obtained by transfection of human embryonic kidney 293 cells using a Retrovirus Packaging Kit Eco (Takara Bio) according to the manufacturer's protocol. The recombinant retrovirus particles containing the target sequence, mock or GnT-V

target sequence (24) as a control, were infected into A549 cells and TGP49 cells, and the geneticine (G418)-resistant clones were selected as a stable transfect. Fut8 activities and GnT-V activities were confirmed in the stable transfectants.

Reverse transcription-polymerase chain reaction (RT-PCR)

Total RNA was purified from cells using the TRIzol reagent (Invitrogen, CA) according to the manufacturer's instructions. One microgram of RNA was reverse-transcribed and amplified using SuperScript™ III (Invitrogen, CA). The following sets of primers were used: VEGFR-2 forward primer, CTG GCA TGG TCT TCT GTG AAG CA; VEGFR-2 reverse primer, AAT ACC AGT GGA TGT GAT GCC G; EGFR forward primer, GTG ATC CAA GCT GTC CCA AT; EGFR reverse primer, GGT GGC ACC AAA GCT GTA TT; TGF–β receptor II (TGFβRII) forward primer, GGA AGC TCA TGG AGT TCA GC; and, TGFβRII reverse primer, GAG CTC TTG AGG TCC CTG TG. The parameters of the PCR program that were used to amplify VEGFR-2 were as follows: 5 minutes initial denaturation at 94 °C; annealing at 60 °C for 1 minute; and, 30 seconds of elongation at 72 °C. This initial cycle was followed by 35 cycles of the following: denaturation at 94 °C for 45 seconds; annealing at 60 °C for 45 seconds, and 2 minutes of elongation at 72 °C followed by 7 minutes of extension at 72 °C. PCR products were visualized in 1.5% ethidium bromide-stained agarose gels. Quantitative real-time PCR analyses of VEGFR-2 and c-fos mRNA expression were performed with an ABI 7900 Sequence Detection System and the 2X SYBR Green PCR Master Mix (ABI, CA). RT was carried out using the following sequence: 42 °C for 60 min; 70 °C for 10 min using random primers; 40 cycles of PCR at 95°C for 15s; and, 60 °C for 1 min with the primers (forward primer, AGCCAGCTCTGGATTTGTGGA; reverse primer, CATGCCCTTAGCCACTTGGAA). The probe for human c-fos was purchased from ABI (Hs00170630_ml). Data were normalized to GAPDH mRNA levels.

Results

Increased apoptosis was observed only in the lungs, and not other organs, of Fut8$^{-/-}$ mice

Pulmonary emphysema is believed to result from the decreased structural integrity of connective tissue due to defective formation or to abnormal proteolysis. The abnormal production of matrix metalloproteinases (MMPs) has been implicated in the induction of emphysema. The TGFβR-mediated signaling pathway is a key pathway in the regulation of ECM protein expression, including expression of MMPs (25). In a previous study, we reported that TGFβ1-mediated signaling was reduced when TGFβR was not α1,6-fucosylated. In addition, the TGFβ1 signaling deficiency was restored by re-introduction of wild type *Fut8* into *Fut8*$^{-/-}$ cells (6). However, the administration of exogenous TGFβ1 only partially rescued the emphysema-like phenotype, suggesting that other mechanisms, besides the TGFβ1-mediated signal pathway, also may be involved in the pathogenesis of emphysema.

Alveolar cell apoptosis is a crucial step in the progression of emphysema. To investigate whether alveolar cell apoptosis is related to emphysema-like changes in the lungs of *Fut8*$^{-/-}$ animals, several mouse tissues were examined using the TUNEL assay. As shown in Fig.1A, apoptotic positive cells localized the alveolar wall were greatly increased in *Fut8*$^{-/-}$ lungs at different ages, in comparison with lungs from littermates of Fut8$^{-/-}$ mice of age-matched normal mice. Interestingly, there were no significant differences in apoptotic cells in the other tissues examined, such as the liver, spleen and kidney, between wild type and *Fut8*$^{-/-}$ mice (Fig.1B).

Down-regulation of VEGFR-2 expression and accumulation of ceramide in the lungs of Fut8$^{-/-}$ mice

Several studies have demonstrated that VEGFR-2-mediated signaling plays an important role in the maintenance of lung alveolar structures. Inhibition of VEGFR-2 has been shown to cause lung cell apoptosis and emphysema (13-17). In the present study, the expression of VEGFR-2 in the lung of wild type and *Fut8*$^{-/-}$ mice was compared. Surprisingly, the expression levels of VEGFR-2 in lungs were significantly lower in *Fut8*$^{-/-}$ mice than in age-matched controls (Fig. 2A and B). We previously reported that loss of the ability to α1,6-fucosylate either EGFR or TGFβRII resulted in a decrease in ligand and receptor-binding, which, in turn, suppressed EGFR- or TGFβRII-mediated signaling, even though receptor expression did not change (6,7). Similar results were observed in the present study. Consistent with the results of the Western blot analysis, immunohistochemical staining showed reduced protein expression in the alveoli and bronchial epithelium of lungs from *Fut8*$^{-/-}$ mice compared with tissue from *Fut8*$^{+/+}$ mice (Fig. 2C). The quantitative analyses also showed that the level of VEGFR-2 expression levels was significantly suppressed in lungs of Fut8-/- mice (right panel of Fig. 2C).

Because ceramide is a prototypic second messenger, which modulates endothelial cell apoptosis, oxidative stress and proteolysis (26-28), it was hypothesized that ceramide up-regulation induces alveolar cell apoptosis. In fact, ceramide up-regulation due to activation of ceramide synthase was observed in VEGFR-2 blockade-induced emphysema. Consistent with the observation, ceramide levels were increased in the lungs of *Fut8*$^{-/-}$ mice, compared with *Fut8*$^{+/+}$ mice (Fig.2D), which was confirmed by a quantitative study (right panel of Fig. 2D). Taken together, these results further support the notion that *Fut8* plays important roles in normal physiologic function and in pathological conditions.

Silencing Fut8 down regulated VEGFR-2 expression

RNA interference (RNAi) knockdown (KD) of the *Fut8* gene in A549 cells was used to confirm the requirement of *Fut8* for VEGFR-2 activity. After retroviral infection, the cells were selected based on their resistance to puromycin as described in the "Materials and methods". The activities of Fut8 were effectively down regulated, compared with those in wild type or mock transfectants (Fig. 3). Next, the expression levels of VEGFR-2 and other receptors were evaluated in these transfectants using RT-PCR, real-time PCR and Western blotting. Silencing *Fut8* significantly decreased expression of VEGFR-2, but not of EGFR, TGFβRII, nor the negative control GAPDH (Fig. 4A). The expression of VEGFR-2, assessed using real-time PCR, was reduced in *Fut8* KD cells to ~10% of expression in mock transfectants and parent cells (Fig. 4B). The Western blot analysis supported the results of real-time PCR (Fig. 4C). Down regulation of VEGFR-2 due to silencing of *Fut8* also was observed in a mouse pancreatic acinar cell carcinoma line, TGP49 (Fig. 4D). It would be worth noting that there were no significant difference in ceramide expression and numbers of apoptotic cell between *Fut8* KD cells and mock cells (data not shown). It is possible that the conditions for cell responses *in vivo* are different from that in cell culture *in vitro*.

Decreased c-Fos expression in Fut8-KD cells

The Fos family of transcription factors plays critical roles in cell proliferation and development. In addition, c-Fos expression is known to be regulated by the VEGFR-2-mediated signal pathway. Therefore, the expression of c-Fos mRNA was examined using RT-PCR in A549 cells. Fut8-knockdown significantly decreased c-Fos expression compared with mock transfectants and parent cells (Fig. 5A). The results from real-time PCR also confirm that the down-regulation of c-fos expression was observed only in the *Fut8* knockdown A549 cells, but not in the mock- or GnT-V-knockdown control cells (Fig. 5B). We previously reported that expression of c-Fos

mRNA extracted from *Fut8*$^{-/-}$ mice was only 35% that of *Fut8*$^{+/+}$ mice (23). These results improve understanding of the underlying mechanism of growth retardation in Fut8-deficient mice.

Discussion

The physiological importance of fucose modification of proteins has been highlighted by the study of human congenital disorders of glycosylation-IIc. These diseases result from a lack of GDP-fucose transporter activity, which in turn causes reduced terminal fucosylation and reduced α1,6-fucosylation. The loss of α1,6-fucosylation has been reported to down-regulate the TGF-β1 receptor, EGF receptor, proteinase-activated receptor and integrin activity, which contributes to emphysema and growth retardation in *Fut8*$^{-/-}$ mice. Previous studies have shown that α1,6-fucosylation plays important roles in ligand-receptor binding, and therefore, in turn in receptor-mediated signaling. Importantly, α1,6-fucosylation does not affect receptor expression. However, in the present study, lack of the *Fut8* gene inhibited VEGFR-2 expression at the level of transcription. Thus, reduction of VEGFR-2 may be considered a second cause of the emphysema-like changes in *Fut8*$^{-/-}$ mice (Fig. 6B). In fact, several studies indicate that enhancement of de novo ceramide species induced by VEGFR blockade is important in the development of emphysema. Consistent with these previous studies, an increase in ceramide expression in the lungs of *Fut8*$^{-/-}$ mice was observed in the present study.

It is well-known that glycoprotein expression can be regulated at posttranslational levels. For example, glycoprotein turnover in the liver can be dramatically accelerated by lectin known as asialoglycoprotein receptors, which bind and internalize glycoproteins lacking or bearing insufficient sialic acid linkages (29). Several studies found that mammalian glycans produced in the Golgi modulate endocytosis of cell-surface glycoproteins, thereby controlling receptor expression and the threshold required for cell signaling (30,31). Very recently Lau et al. used both

computational modeling and experimental data in T cells and in epithelial cells, to show that galectin-binding to N-glycan on membrane glycoproteins enhances surface residency, dependent on N-glycan number and on N-glycan GlcNAc-branching activity, which, in turn, are affected by the supply of UDP-GlcNAc (32). The transcriptional control of the VEGFR-2 seems to be complex. Hypoxia increases VEGFR-2 gene expression (33), while tumor necrosis factor-α down-regulates it (34). The precise mechanism of down-regulation of VEGFR-2 expression in lungs of *Fut8*-deficient mice or in *Fut8*-knockdown cells remains unclear, but this observation should be quite useful for understanding the molecular mechanisms that lead to development of emphysema in humans.

mRNA expression of c-Fos in *Fut8*$^{-/-}$ tissues was lower than in wild type tissues, as described previously (23). Consistent with these previously reported results, the present study demonstrated that c-Fos expression was down regulated by repression of *Fut8* in A549 cells, strongly suggesting that Fut8 plays an important role in c-Fos expression. Since c-Fos has been proposed to participate in regulation of cell proliferation and development (35,36), the down regulation of c-Fos expression in *Fut8*$^{-/-}$ mice may be a newly identified mechanism of growth retardation. Although the expression of c-Fos can be regulated by the VEGFR-mediated signaling pathway (37), other effectors of c-Fos expression induction cannot be excluded. For example, EGF can also induce c-Fos via extracellular signal-regulated kinase-dependent and PKC-dependent pathways (38). The loss of α1,6-fucose resulted in down-regulation of EGFR-mediated signaling as described previously (7,23). Therefore, the lower levels of c-Fos expression in *Fut8*-deficient cells may be due to down-regulation of several growth factor receptor-mediated signaling pathways via both functional and expressional levels.

Pulmonary emphysema is a major consequence of COPD, with a worldwide epidemic looming as more people become addicted to cigarettes. The treatment options for patients in the later

stages of the disease, other than oxygen, are limited. Therefore, development of new treatments requires improved understanding of the biological basis of this disease. To date, hypotheses based on protease-anti-protease imbalance and on inflammation have been most relevant, however, the importance of VEGFR-2 signaling also has recently been shown. The present study demonstrated that deficiency of *Fut8* profoundly blocks VEGFR-2 expression in *Fut8*$^{-/-}$ mice and cells, identifying another cause of emphysema. Similar defects may be responsible for some cases of human emphysema.

Acknowledgments

This work was partly supported by Core Research for Evolutional Science and Technology (CREST), Japan Science and Technology Agency (JST) and the Academic Frontier Project for Private Universities from the Ministry of Education, Culture, Sports, Science and Technology of Japan, and the core to core program (JSPS), and Takeda Science Foundation, Japan.

Abbreviations

Fut8: α1,6-fucosyltransferase; VEGFR-2: vascular endothelial cell growth factor receptor-2; DMEM, Dulbecco's modified Eagle's medium; PBS, phosphate buffered saline; FBS, fetal bovine serum; TUNEL: terminal transferase dUTP nick end labeling

CONFLICT OF INTEREST

None declared.

References

1. Wilson, J.R., Williams, D. and Schachter, H. (1976) The control of glycoprotein synthesis: N-acetylglucosamine linkage to a mannose residue as a signal for the attachment of L-fucose to the asparagine-linked N-acetylglucosamine residue of glycopeptide from alpha1-acid glycoprotein. *Biochem Biophys Res Commun*, **72**, 909-916.
2. Miyoshi, E., Noda, K., Yamaguchi, Y., Inoue, S., Ikeda, Y., Wang, W., Ko, J.H., Uozumi, N., Li, W. and Taniguchi, N. (1999) The alpha1-6-fucosyltransferase gene and its biological significance. *Biochim Biophys Acta*, **1473**, 9-20.
3. Noda, K., Miyoshi, E., Gu, J., Gao, C.X., Nakahara, S., Kitada, T., Honke, K., Suzuki, K., Yoshihara, H., Yoshikawa, K., Kawano, K., Tonetti, M., Kasahara, A., Hori, M., Hayashi, N. and Taniguchi, N. (2003) Relationship between elevated FX expression and increased production of GDP-L-fucose, a common donor substrate for fucosylation in human hepatocellular carcinoma and hepatoma cell lines. *Cancer Res*, **63**, 6282-6289.
4. Shields, R.L., Lai, J., Keck, R., O'Connell, L.Y., Hong, K., Meng, Y.G., Weikert, S.H. and Presta, L.G. (2002) Lack of fucose on human IgG1 N-linked oligosaccharide improves binding to human Fcgamma RIII and antibody-dependent cellular toxicity. *J Biol Chem*, **277**, 26733-26740.
5. Shinkawa, T., Nakamura, K., Yamane, N., Shoji-Hosaka, E., Kanda, Y., Sakurada, M., Uchida, K., Anazawa, H., Satoh, M., Yamasaki, M., Hanai, N and Shitara, K. (2003) The absence of fucose but not the presence of galactose or bisecting N-acetylglucosamine of human IgG1 complex-type oligosaccharides shows the critical role of enhancing antibody-dependent cellular cytotoxicity. *J Biol Chem*, **278**, 3466-3473.
6. Wang, X., Inoue, S., Gu, J., Miyoshi, E., Noda, K., Li, W., Mizuno-Horikawa, Y., Nakano, M., Asahi, M., Takahashi, M., Uozumi, N., Ihara, S., Lee, S.H., Ikeda, Y., Yamaguchi, Y., Aze, Y., Tomiyama, Y., Fujii, J., Suzuki, K., Kondo, A., Shapiro, S.D., Lopez-Otin, C., Kuwaki, T., Okabe, M., Honke, K. and Taniguchi, N. (2005) Dysregulation of TGF-beta1 receptor activation leads to abnormal lung development and emphysema-like phenotype in core fucose-deficient mice. *Proc Natl Acad Sci U S A*, **102**, 15791-15796.
7. Wang, X., Gu, J., Ihara, H., Miyoshi, E., Honke, K. and Taniguchi, N. (2006) Core fucosylation regulates epidermal growth factor receptor-mediated intracellular signaling. *J Biol Chem*, **281**, 2572-2577.

8. Zhao, Y., Itoh, S., Wang, X., Isaji, T., Miyoshi, E., Kariya, Y., Miyazaki, K., Kawasaki, N., Taniguchi, N. and Gu, J. (2006) Deletion of core fucosylation on alpha3beta1 integrin down-regulates its functions. *J Biol Chem*, **281**, 38343-38350.

9. Kondo, A., Li, W., Nakagawa, T., Nakano, M., Koyama, N., Wang, X., Gu, J., Miyoshi, E. and Taniguchi, N. (2006) From glycomics to functional glycomics of sugar chains: Identification of target proteins with functional changes using gene targeting mice and knock down cells of FUT8 as examples. *Biochim Biophys Acta*, **1764**, 1881-1889.

10. Taniguchi, N., Miyoshi, E., Gu, J., Honke, K. and Matsumoto, A. (2006) Decoding sugar functions by identifying target glycoproteins. *Curr Opin Struct Biol*, **16**, 561-566.

11. Hautamaki, R.D., Kobayashi, D.K., Senior, R.M. and Shapiro, S.D. (1997) Requirement for macrophage elastase for cigarette smoke-induced emphysema in mice. *Science*, **277**, 2002-2004.

12. Morris, D.G., Huang, X., Kaminski, N., Wang, Y., Shapiro, S.D., Dolganov, G., Glick, A. and Sheppard, D. (2003) Loss of integrin alpha(v)beta6-mediated TGF-beta activation causes Mmp12-dependent emphysema. *Nature*, **422**, 169-173.

13. Kasahara, Y., Tuder, R.M., Cool, C.D., Lynch, D.A., Flores, S.C. and Voelkel, N.F. (2001) Endothelial cell death and decreased expression of vascular endothelial growth factor and vascular endothelial growth factor receptor 2 in emphysema. *Am J Respir Crit Care Med*, **163**, 737-744.

14. Kasahara, Y., Tuder, R.M., Taraseviciene-Stewart, L., Le Cras, T.D., Abman, S., Hirth, P.K., Waltenberger, J. and Voelkel, N.F. (2000) Inhibition of VEGF receptors causes lung cell apoptosis and emphysema. *J Clin Invest*, **106**, 1311-1319.

15. Petrache, I., Natarajan, V., Zhen, L., Medler, T.R., Richter, A., Berdyshev, E.V. and Tuder, R.M. (2006) Ceramide causes pulmonary cell apoptosis and emphysema: a role for sphingolipid homeostasis in the maintenance of alveolar cells. *Proc Am Thorac Soc*, **3**, 510.

16. Petrache, I., Natarajan, V., Zhen, L., Medler, T.R., Richter, A.T., Cho, C., Hubbard, W.C., Berdyshev, E.V. and Tuder, R.M. (2005) Ceramide upregulation causes pulmonary cell apoptosis and emphysema-like disease in mice. *Nat Med*, **11**, 491-498.

17. Tang, K., Rossiter, H.B., Wagner, P.D. and Breen, E.C. (2004) Lung-targeted VEGF inactivation leads to an emphysema phenotype in mice. *J Appl Physiol*, **97**, 1559-1566; discussion 1549.

18. Suzuki, M., Betsuyaku, T., Nagai, K., Fuke, S., Nasuhara, Y., Kaga, K., Kondo, S., Hamamura, I., Hata, J., Takahashi, H. and Nishimura, M. (2008) Decreased airway expression of vascular endothelial growth factor in cigarette smoke-induced emphysema in mice and COPD patients. *Inhal Toxicol*, **20**, 349-359.

19. Tuder, R.M., Petrache, I., Elias, J.A., Voelkel, N.F. and Henson, P.M. (2003) Apoptosis and emphysema: the missing link. *Am J Respir Cell Mol Biol*, **28**, 551-554.

20. Alon, T., Hemo, I., Itin, A., Pe'er, J., Stone, J. and Keshet, E. (1995) Vascular endothelial growth factor acts as a survival factor for newly formed retinal vessels and has implications for retinopathy of prematurity. *Nat Med*, **1**, 1024-1028.

21. Gerber, H.P., McMurtrey, A., Kowalski, J., Yan, M., Keyt, B.A., Dixit, V. and Ferrara, N. (1998) Vascular endothelial growth factor regulates endothelial cell survival through the phosphatidylinositol 3'-kinase/Akt signal transduction pathway. Requirement for Flk-1/KDR activation. *J Biol Chem*, **273**, 30336-30343.

22. Uozumi, N., Teshima, T., Yamamoto, T., Nishikawa, A., Gao, Y.E., Miyoshi, E., Gao, C.X., Noda, K., Islam, K.N., Ihara, Y., Fujii, S., Shiba, T. and Taniguchi, N. (1996) A fluorescent assay method for GDP-L-Fuc:N-acetyl-beta-D-glucosaminide alpha 1-6fucosyltransferase activity, involving high performance liquid chromatography. *J Biochem (Tokyo)*, **120**, 385-392.

23. Li, W., Nakagawa, T., Koyama, N., Wang, X., Jin, J., Mizuno-Horikawa, Y., Gu, J., Miyoshi, E., Kato, I., Honke, K., Taniguchi, N. and Kondo, A. (2006) Down-regulation of trypsinogen expression is associated with growth retardation in alpha1,6-fucosyltransferase-deficient mice: attenuation of proteinase-activated receptor 2 activity. *Glycobiology*, **16**, 1007-1019.

24. Inamori, K., Gu, J., Ohira, M., Kawasaki, A., Nakamura, Y., Nakagawa, T., Kondo, A., Miyoshi, E., Nakagawara, A. and Taniguchi, N. (2006) High expression of N-acetylglucosaminyltransferase V in favorable neuroblastomas: Involvement of its effect on apoptosis. *FEBS Lett*, **580**, 627-632.

25. Massague, J., Blain, S.W. and Lo, R.S. (2000) TGFbeta signaling in growth control, cancer, and heritable disorders. *Cell*, **103**, 295-309.

26. Hannun, Y.A. and Luberto, C. (2000) Ceramide in the eukaryotic stress response. *Trends Cell Biol*, **10**, 73-80.

27. Hannun, Y.A. and Obeid, L.M. (2002) The Ceramide-centric universe of lipid-mediated cell regulation: stress encounters of the lipid kind. *J Biol Chem*, **277**, 25847-25850.

28. Reunanen, N., Westermarck, J., Hakkinen, L., Holmstrom, T.H., Elo, I., Eriksson, J.E. and Kahari, V.M. (1998) Enhancement of fibroblast collagenase (matrix metalloproteinase-1) gene expression by ceramide is mediated by extracellular signal-regulated and stress-activated protein kinase pathways. *J Biol Chem*, **273**, 5137-5145.

29. Ashwell, G. and Harford, J. (1982) Carbohydrate-specific receptors of the liver. *Annu Rev Biochem*, **51**, 531-554.

30. Ohtsubo, K., Takamatsu, S., Minowa, M.T., Yoshida, A., Takeuchi, M. and Marth, J.D. (2005) Dietary and genetic control of glucose transporter 2 glycosylation promotes insulin secretion in suppressing diabetes. *Cell*, **123**, 1307-1321.

31. Partridge, E.A., Le Roy, C., Di Guglielmo, G.M., Pawling, J., Cheung, P., Granovsky, M., Nabi, I.R., Wrana, J.L. and Dennis, J.W. (2004) Regulation of cytokine receptors by Golgi N-glycan processing and endocytosis. *Science*, **306**, 120-124.

32. Lau, K.S., Partridge, E.A., Grigorian, A., Silvescu, C.I., Reinhold, V.N., Demetriou, M. and Dennis, J.W. (2007) Complex N-glycan number and degree of branching cooperate to regulate cell proliferation and differentiation. *Cell*, **129**, 123-134.

33. Tuder, R.M., Flook, B.E. and Voelkel, N.F. (1995) Increased gene expression for VEGF and the VEGF receptors KDR/Flk and Flt in lungs exposed to acute or to chronic hypoxia. Modulation of gene expression by nitric oxide. *J Clin Invest*, **95**, 1798-1807.

34. Patterson, C., Perrella, M.A., Endege, W.O., Yoshizumi, M., Lee, M.E. and Haber, E. (1996) Downregulation of vascular endothelial growth factor receptors by tumor necrosis factor-alpha in cultured human vascular endothelial cells. *J Clin Invest*, **98**, 490-496.

35. Angel, P. and Karin, M. (1991) The role of Jun, Fos and the AP-1 complex in cell-proliferation and transformation. *Biochim Biophys Acta*, **1072**, 129-157.

36. Jochum, W., Passegue, E. and Wagner, E.F. (2001) AP-1 in mouse development and tumorigenesis. *Oncogene*, **20**, 2401-2412.

37. Holmes, D.I. and Zachary, I. (2004) Placental growth factor induces FosB and c-Fos gene expression via Flt-1 receptors. *FEBS Lett*, **557**, 93-98.

38. Chen, D.B. and Davis, J.S. (2003) Epidermal growth factor induces c-fos and c-jun mRNA via Raf-1/MEK1/ERK-dependent and -independent pathways in bovine luteal cells. *Mol Cell Endocrinol*, **200**, 141-154.

Figure legends

Fig.1. Tissue sections stained using the TUNEL technique. The lung sections from mice at different ages (embryo 12.5-day and 18.5-day, postnatal 10-day, 18-day, 8-week and 4-month old) (*A*), and other tissues such as liver, spleen, heart and kidney of postnatal 18-day-old (*B*) of *Fut8*$^{-/-}$ and *Fut8*$^{+/+}$ mice were subjected to the TUNEL assay. The *Fut8*$^{+/+}$ mice were littermates of Fut8$^{-/-}$ mice. TUNEL-staining was performed with DeadEnd™ Colorimetric TUNEL System as described in the "Materials and methods". Arrowheads indicate apoptotic cells.

Fig.2. Decreased VEGFR-2 expression levels and increased ceramide levels in lungs of *Fut8*$^{-/-}$ mice. *A*: VEGFR-2 expression levels were assayed using Western blot (WB) in lung homogenates in *Fut8*$^{-/-}$ and *Fut8*$^{+/+}$ mice of different ages. The expression levels of EGFR, TβRII and β-actin were used as controls. *B*: The quantitative data were expressed as ratios of VEGFR-2/β-actin. The density of bands for VEGFR-2 and β-actin, in which β-actin expression served as the control, was measured using ImageJ software. *C*: Decreased VEGFR-2 expression levels in lungs of *Fut8*$^{-/-}$ mice compared with that in *Fut8*$^{+/+}$ mice examined by immunohistochemical staining with anti-VEGFR-2 antibody. Fifty dots of equivalent area (228 mm^2) were stochastically selected and examined for quantitative analyses of VEGFR-2 (right panel). Arrowheads indicate stronger positive staining. a: alveoli; b: bronchial epithelium. *D*: Increased ceramide expression levels in the lung of *Fut8*$^{-/-}$ mice, compared with that in *Fut8*$^{+/+}$ mice examined by immunohistochemical staining with anti-ceramide antibody. Nine dots of equivalent area (280 mm^2) were selected and examined for quantitative analyses of ceremide (right panel). Arrowheads indicate strong positive staining. p7D: postnatal 7-day-old; p18D: postnatal 18-day; p8w: postnatal 8-week-old. Density was measured using ImageJ software. The wild-type mice were littermates of Fut8$^{-/-}$ mice.

Fig.3. Silencing effects of siRNA on Fut8 activity. The *Fut8* gene in human alveolar epithelial cell carcinoma A549 cell was knocked down using the siRNA technique as described in the "Materials and methods". *A*: HPLC elution profiles of GnGn-Asn-PAPB substrate (S) and the Fut8 product (P). The large peak at 10 min shows the un-reacted substrates, the peak at 17 min indicated by the arrow is the product. *B*: Quantification of Fut8 activity. The Fut8 specific activity (pmol product/mg lysate/h) in wild type A549 cells was set to 100. *KD*, *Fut8* knockdown cells.

Fig.4. Decreased VEGFR-2 expression levels in *Fut8* knockdown cells. The expression levels of VEGFR-2 in A549 cells were examined by RT-PCR (*A*) and real-time PCR (*B*). The expression levels of TβRII, EGFR and GAPDH were used as controls. *C*: The protein levels of VEGFR-2 were examined by Western blot of the immunoprecipitates of VEGFR-2 from 400 μg cell lysates. The amount of cell lysates was confirmed by Western blot of EGFR. *D*: The expression levels of VEGFR-2 in TPG49 cells were examined by RT-PCR. The expression level of β-actin was used as the control. *KD*, *Fut8* knockdown cells.

Fig.5. Down regulation of c-Fos expression in Fut8 knockdown cells. c-Fos expression levels were examined by RT-PCR (*A*) and real-time PCR (*B*). The same amount of cDNA was used, as confirmed by GAPDH expression. *KD*, Fut8 knockdown cells.

Fig.6. Two possible mechanisms are involved in emphysema-like changes in *Fut8*$^{-/-}$ mice. *A*: Reaction pathway for the biosynthesis of core fucose by *Fut8*. *Man*, mannose; *Fuc*, fucose; *GDP-Fuc*, guanosinediphospho-fucopyranoside; *Asn*, asparagine. *B*: Pulmonary emphysema is believed to result from the decreased structural integrity of connective tissues due to defective in their formation or to abnormal proteolysis. The lungs of *Fut8*$^{-/-}$ mice apparently displayed generalized air space enlargement and dilated alveolar ducts, compared with *Fut8*$^{+/+}$ mice. One possible mechanism is that the decreased response to TGFβ1 stimulation (the left scheme) is due to reduced binding of TGFβ1 to its receptor TGFβRII, resulting in enhanced expression of MMPs in *Fut8*$^{-/-}$ mice. The other mechanism, first described in the present study, is shown in the right scheme. In the present study, *Fut8* was required for VEGFR-2 expression *in vivo* and *in vitro*. Down regulation of VEGFR-2 expression may enhance ceramide expression, which contributes to the pathogenesis of emphysema. The dashed line indicates the obscure mechanism for the decreased VEGFR expression in *Fut8*$^{-/-}$ mice.

Fig.1 Wang, et.al.

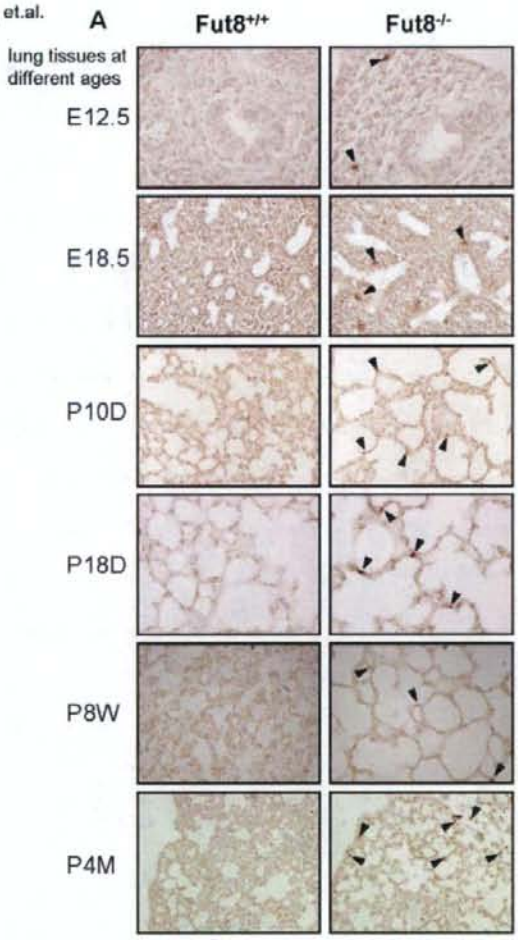

Fig.1 Wang, et.al.